Clim Dyn
DOI 10.1007/s00382-015-2816-6

Twenty-first century probabilistic projections of precipitation over Ontario, Canada through a regional climate model ensemble

Xiuquan Wang[1] · **Guohe Huang**[2,3] · **Jinliang Liu**[4]

Received: 22 March 2015 / Accepted: 24 August 2015

Abstract In this study, probabilistic projections of precipitation for the Province of Ontario are developed through a regional climate model ensemble to help investigate how global warming would affect its local climate. The PRECIS regional climate modeling system is employed to perform ensemble simulations, driven by a set of boundary conditions from a HadCM3-based perturbed-physics ensemble. The PRECIS ensemble simulations are fed into a Bayesian hierarchical model to quantify uncertain factors affecting the resulting projections of precipitation and thus generate probabilistic precipitation changes at grid point scales. Following that, reliable precipitation projections throughout the twenty-first century are developed for the entire province by applying the probabilistic changes to the observed precipitation. The results show that the vast majority of cities in Ontario are likely to suffer positive changes in annual precipitation in 2030, 2050, and 2080 s in comparison to the baseline observations. This may suggest that the whole province is likely to gain more precipitation throughout the twenty-first century in response to global warming. The analyses on the projections of seasonal precipitation further demonstrate that the entire province is likely to receive more precipitation in winter, spring, and autumn throughout this century while summer precipitation is only likely to increase slightly in 2030 s and would decrease gradually afterwards. However, because the magnitude of projected decrease in summer precipitation is relatively small in comparison with the anticipated increases in other three seasons, the annual precipitation over Ontario is likely to suffer a progressive increase throughout the twenty-first century (by 7.0 % in 2030 s, 9.5 % in 2050 s, and 12.6 % in 2080 s). Besides, the degree of uncertainty for precipitation projections is analyzed. The results suggest that future changes in spring precipitation show higher degree of uncertainty than other seasons, resulting in more uncertainties in annual precipitation projections.

Keywords Global warming · Regional climate change · Precipitation projections · Climate ensemble · Ontario

1 Introduction

Global warming caused by the increase in greenhouse gas concentrations is likely to alter the planet's hydrologic cycle, and would further lead to substantial changes in the amount, intensity, and spatial distribution of precipitation (Allan and Soden 2008; Chou et al. 2009; Fowler and Hennessy 1995; Hulme et al. 1998; Trenberth 2011; Wentz et al. 2007). These changes may pose a number of serious

Electronic supplementary material The online version of this article (doi:10.1007/s00382-015-2816-6) contains supplementary material, which is available to authorized users.

✉ Guohe Huang
huang@iseis.org

Xiuquan Wang
xiuquan.wang@gmail.com

[1] Institute for Energy, Environment and Sustainable Communities, University of Regina, Regina, SK S4S 0A2, Canada

[2] Institute for Energy, Environment and Sustainability Research, UR-NCEPU, University of Regina, Regina, SK S4S 0A2, Canada

[3] Institute for Energy, Environment and Sustainability Research, UR-NCEPU, North China Electric Power University, Beijing 102206, China

[4] Department of Earth and Space Science and Engineering, York University, Toronto, ON M3J 1P3, Canada

Published online: 08 September 2015

risks on natural and human systems on all continents and in the ocean (IPCC 2014; Jordan et al. 2014). For example, changing precipitation or melting snow or ice are altering hydrological systems in many regions and may further affect water resources in terms of quantity and quality (e.g., Akhtar et al. 2008; Baron et al. 2013; Christensen and Lettenmaier 2007; Grafton et al. 2013; Ling et al. 2014; Paerl and Paul 2012; Piao et al. 2010; Wang et al. 2014a), extreme weather events (e.g., floods and droughts) are occurring more frequent in recent years and may lead to severe and irreversible impacts on human and ecosystems (e.g., Aldous et al. 2011; Dai 2011; Hirabayashi et al. 2013; Ma et al. 2014; Marengo et al. 2013; Schiermeier 2011; Wang et al. 2014d; Yang et al. 2012). Assessing the potential impacts of global warming on precipitation thus becomes one of the major concerns for decision makers and resources managers to help develop scientifically-informed policies or strategies against the changing climate (Cross et al. 2012; Ford et al. 2011; Hoffmann and Sgrò 2011).

Precipitation is highly spatially variable because it is not only affected by the global hydrologic cycle, but also influenced by local topography, land cover, inland waters, coastlines, and many other regional details (Bárdossy and Pegram 2013; Sanchez-Moreno et al. 2014; Senatore et al. 2014; Um et al. 2011). Global climate models (GCMs) can hardly account for the spatial variability because they usually run at the global scale with a coarse resolution of 150-300 km. Further downscaling to the GCM outputs is required to generate future climate projections at finer resolutions for supporting climate change impact assessment at regional scales (Wang et al. 2014c). In general, downscaling techniques are classified into statistical downscaling and dynamical downscaling. Statistical downscaling involves the development of quantitative relationships between large-scale atmospheric variables and local weather variables such as temperature and precipitation (Hewitson and Crane 1996; Wilby and Wigley 1997). Owing to its easier implementation and lower computational requirements than dynamical downscaling, statistical downscaling has been widely used in climate research community (e.g., Abatzoglou and Brown 2012; Feddersen and Andersen 2005; He et al. 2011; Korhonen et al. 2014; Themeßl et al. 2012; Wang et al. 2013). But, statistical downscaling methods have many limitations and are subject to a number of widely-known assumptions on the underlying probabilistic model, parameter stability, as well as temporal dependence which are not always satisfied in the context of climate change (Estrada et al. 2013; Wang et al. 2014e). In contrast, dynamical downscaling is usually implemented by nesting fine-resolution regional climate models (RCMs) into GCMs in order to account for the sub-GCM grid scale processes in a physically-based way (Feser et al. 2011). RCMs are developed with the same laws of physics as described in GCMs and can be used to simulate the local climate system with provision of a large number of climate variables at fine spatial resolutions (in the order of 10 km). Dynamical downscaling through RCMs thus have received increasing attention of climate impact researchers in the past few years (e.g., Heinrich et al. 2014; Larsen et al. 2014; Nikulin et al. 2012; Pielke and Wilby 2012; Teutschbein and Seibert 2012).

As the biggest economy in Canada, the Province of Ontario is experiencing many consequences caused by or associated with climate change, such as frequent and intense heat waves, floods, droughts, and wind gust (MoE 2011a, b). Planning of mitigation and adaptation strategies against the changing climate, which requires a better understanding of future climate outcomes over the province in the context of global warming, is of great interest to local policy makers, stakeholders, and development practitioners. Therefore, as an extension of our previous efforts on probabilistic temperature projections (Wang et al. 2014b, e, 2015), this paper aims to develop high-resolution precipitation projections for the Province of Ontario through a regional climate model ensemble to help investigate the potential impacts of global warming on precipitation at regional scales. Specifically, we will first employ the PRECIS model to perform ensemble simulations of the local climate over Ontario, driven by a set of boundary conditions from a HadCM3-based perturbed-physics ensemble. The PRECIS ensemble simulations will be then fed into a Bayesian hierarchical model (Wang et al. 2014b) to quantify uncertain factors affecting the resulting projections of precipitation and thus generate probabilistic precipitation changes at grid point scales. By applying the probabilistic changes to the observed precipitation, we will develop reliable precipitation projections throughout the twenty-first century for the entire province to provide helpful information for assessing the potential effects of climate change in the context of Ontario.

2 Methodology

2.1 Model description and experimental design

In this study, we use the PRECIS regional climate modeling system developed at the UK Met Office Hadley Centre to perform high-resolution climate simulations for the Province of Ontario. The PRECIS is a flexible, easy-to-use and computationally inexpensive RCM designed to provide detailed climate scenarios. It can be applied easily to any area of the globe to generate detailed climate change projections, with the provision of a simple user interface as well as a visualization and data-processing package. The PRECIS is able to run at two different

horizontal resolutions: 0.44° (approximately 50 km) and 0.22° (approximately 25 km), with 19 vertical levels using a hybrid coordinate system (Wilson et al. 2011). The PRECIS is a comprehensive physical model with consideration of both the atmosphere and land surface components of the climate system, and thus is capable of representing the important physical processes within the climate system, such as dynamical flow, atmospheric sulphur cycle, clouds and precipitation, radiative processes, and the interactions between land surface and deep soil (Jones et al. 2004).

The PRECIS model requires surface boundary conditions and lateral boundary conditions at its edges, but there is no prescribed constant at the upper boundary of the model (except for the input of solar radiation). Surface boundary conditions are only required over ocean and inland water where the model needs timeseries of surface temperatures and ice extents. Lateral boundary conditions provide the necessary dynamical atmospheric information at the latitudinal and longitudinal edges of the model domain (e.g., surface pressure, winds, temperature, and humidity). Lateral boundary conditions are updated every 6 h in the PRECIS model while surface boundary conditions are updated every day (Jones et al. 2004). In this paper, we derive boundary conditions from a HadCM3-based perturbed physics ensemble (known as QUMP, available at: http://www.metoffice.gov.uk/precis/qump) under the SRES A1B emission scenario to drive the PRECIS simulations over Ontario. The QUMP consists of 17 members and is developed by the Hadley Centre to allow users to generate an ensemble of high-resolution regional climate projections (Collins et al. 2006). Downscaling the 17-member PPE ensemble with PRECIS would require very large inputs of computing resources, data storage, and data analyses. In order to explore the range of uncertainties while minimizing these requirements, we select 5 members (i.e., HadCM3Q0, Q3, Q10, Q13, and Q15) from the QUMP ensemble according to the Hadley Centre's recommendation (McSweeney and Jones 2010). HadCM3Q0 is first selected as it is the standard, unperturbed model using the original parameter settings as applied in the atmospheric component of HadCM3. Selection of the remaining four members is based on: (a) their performances in simulating the climate of the present day, to ensure that the selected members can represent the climate of the region of interest reasonably, and (b) the range or spread of future outcomes, in order to ensure that the selected members can sample the full range of outcomes simulated by the 17-member ensemble (McSweeney et al. 2012). More details about the physical parameter settings of the selected 5 members can be found in the papers of Murphy et al. (2004), Barnett et al. (2006), and Collins et al. (2006). In this study, we carry out the PRECIS ensemble simulations for the Province of Ontario (shown Fig. 1) in a continuous run from 1950 to 2099 with a resolution of 25 km.

2.2 Ensemble validation

In this study, we use the 10-km gridded climate dataset provided by the National Land and Water Information Service (NLWIS), Agriculture and Agri-Food, Canada to validate the capability of PRECIS ensemble simulations in reproducing the observed precipitation of current climate in the context of Ontario. The NLWIS dataset is interpolated from daily Environment Canada climate station observations through a thin plate smoothing spline surface fitting method as implemented by ANUSPLIN V4.3 (NLWIS 2007). Observations from the NLWIS dataset are available for the period of 1961–2003, here we extract the data for 1961–1990 (hereinafter referred to as baseline period) to represent the observations of current climate. The NLWIS dataset is regridded to the 25-km grids specified by the PRECIS model such that the validation and undermentioned probabilistic analysis can be conducted at the same spatial resolution.

Instead of comparing each member of the ensemble with the NLWIS dataset, we calculate the difference between ensemble projections and observations (denoted as D) to measure the ensemble performance in capturing the observed precipitation of current climate, as follows:

$$D = \begin{cases} \frac{P_{min} - P_{obs}}{P_{obs}} \times 100\,\% & \text{if } P_{obs} < P_{min} \\ 0 & \text{if } P_{min} \le P_{obs} \le P_{max} \\ \frac{P_{max} - P_{obs}}{P_{obs}} \times 100\,\% & \text{if } P_{obs} > P_{max} \end{cases} \quad (1)$$

where P_{obs} indicates the observed precipitation for current climate which can be derived from the NLWIS dataset, P_{min} and P_{max} represent the minimum and maximum precipitation simulated by the PRECIS ensemble. Positive values of D indicate overestimation to the observed precipitation while negative values mean underestimation.

2.3 Probabilistic projections of precipitation

Ensemble projections of future climate change are usually presented in a probabilistic way based upon a variety of statistical methods (e.g., Giorgi and Mearns 2002, 2003; Tebaldi et al. 2005), such that more helpful information can be obtained reasonably for supporting climate change impact assessment and the subsequent policy making. Each possible outcome of future climate change will come with a specific level of occurrence (i.e., probability), it thus allows for planning appropriate adaptation strategies in advance by balancing the tradeoff between adapting costs and potential damages of climate change for a specific region

Fig. 1 Elevation distribution of the study area

or community at different probabilistic levels. In order to synthesize the PRECIS ensemble simulations and interpret them into policy-relevant information, here we introduce a Bayesian hierarchical model (Wang et al. 2014b) to help develop probabilistic projections of annual and seasonal precipitation over Ontario. In detail, future precipitation scenarios (denoted as P_{fut}) can be calculated by:

$$P_{fut} = P_{obs} \times (1 + \Delta_{pro}) \tag{2}$$

where Δ_{pro} means the projected percentage change in 30-year mean annual or seasonal precipitation at a given grid cell by the PRECIS ensemble simulations. Note that P_{obs} and Δ_{pro} will be dealt with in a grid-by-grid fashion such that future precipitation projections for all grid cells over Ontario can be developed. We regard Δ_{pro} as a random variable because it is unknown or uncertain at this stage. Thus, Δ_{pro} can be estimated by the difference between the true value of precipitation for future climate (denoted as ν) and that of current climate (denoted as μ), as follows:

$$\Delta_{pro} = \frac{\nu - \mu}{\mu} \times 100\,\% \tag{3}$$

where ν and μ are treated as random variables with uniform prior distributions on the real line (i.e., $[0, +\infty]$). Posterior distributions for ν and μ can be derived through Bayesian inference theory. Assumptions on the non-informative priors of all unknown parameters and the derivation of their posteriors are detailed in the paper of Wang et al. (2014b). The posterior distributions for ν and μ are expressed as follows:

$$\mu \sim N\left(\frac{\sum_{i=1}^{n}\left[\lambda_i x_i - \theta\beta\lambda_i(y_i - \nu - \beta x_i)\right] + \lambda_0 x_0}{\lambda_0 + \sum_{i=1}^{n}\lambda_i(1+\theta\beta^2)}, \frac{1}{\lambda_0 + \sum_{i=1}^{n}\lambda_i(1+\theta\beta^2)}\right) \tag{4}$$

$$\nu \sim N\left(\frac{\sum_{i=1}^{n}\lambda_i\left[y_i - \beta(x_i - \mu)\right]}{\sum_{i=1}^{n}\lambda_i}, \frac{1}{\theta\sum_{i=1}^{n}\lambda_i}\right) \tag{5}$$

where n means the total number of members in the PRECIS ensemble (i.e., $n = 5$); x_i and y_i represent the simulated precipitation for current and future climate by the ith PRECIS run; x_0 indicates the biased observations of precipitation for current climate with consideration of random errors and systematic errors due to different measurement

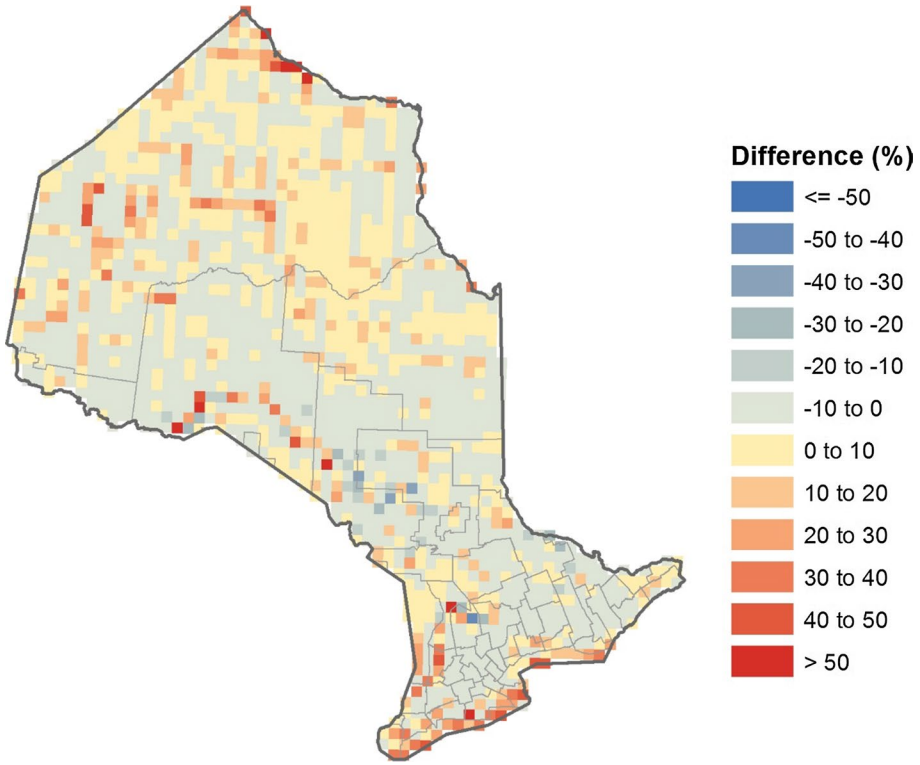

Fig. 2 Difference between the simulated annual precipitation and the observed one for the baseline period

platforms and practices (Wang et al. 2014b). The remaining parameters (i.e., λ_0, λ_i, β, θ) are used to reflect various uncertainties associated with the PRECIS ensemble simulations, and their definitions are detailed in the paper of Wang et al. (2014b). An empirical estimate of the posterior distribution for Δ_{pro} is obtained through a Gibbs-based Markov chain Monte Carlo (MCMC) implementation to the proposed model (Wang et al. 2014b), thus the probabilistic precipitation scenarios (i.e., P_{fut}) can be generated according to Eq. (2).

2.4 Interpretation of probabilistic projections

Due to our limited knowledge of the climate system and the resulting imperfectness of climate models, we can give only plausible outcomes for future climate. That is why we develop probabilistic projections by assigning a probability to each possible outcome for future climate, instead of giving a single answer, to help with making robust adaptation decisions (Murphy et al. 2009). Instead of providing an absolute probability to describe the occurrence of each possible outcome, we use the cumulative distribution function (CDF) in this study to define the probability of future projections of precipitation being less than or greater than a given amount. Specifically, we use a cumulative probability of 90 % to describe probabilistic projections by saying that the projected precipitation is very likely to be less than or very unlikely to be greater than a given value; we use a cumulative probability of 10 % to indicate very likely to be greater than or very unlikely to be less than; and we regard the value with a cumulative probability of 50 % as the central estimate of future projections (also known as the median of the distribution). For convenience, we use the term of probability rather than cumulative probability in the rest of this paper.

3 Results

3.1 Validation of the PRECIS ensemble

To validate the capability of the PRECIS ensemble in capturing the spatial patterns of precipitation over Ontario, we extract the simulated annual and seasonal precipitation in the baseline period from the five member runs and calculate their differences from the observations according to Eq. (1). Figure 2 shows the difference map of annual precipitation. It is clear that most of grid cells within the domain of Ontario present little differences (ranging between −10 and 10 %) from the observations, while the remainder are likely to manifest positive differences higher than 10 %. The differences in annual precipitation at all grid cells also demonstrate a slight but still distinguishable spatial distribution along with the latitude. Specifically, most of grid cells in the south show negative differences within [−10, 0] % while the grid cells in the north are largely with positive

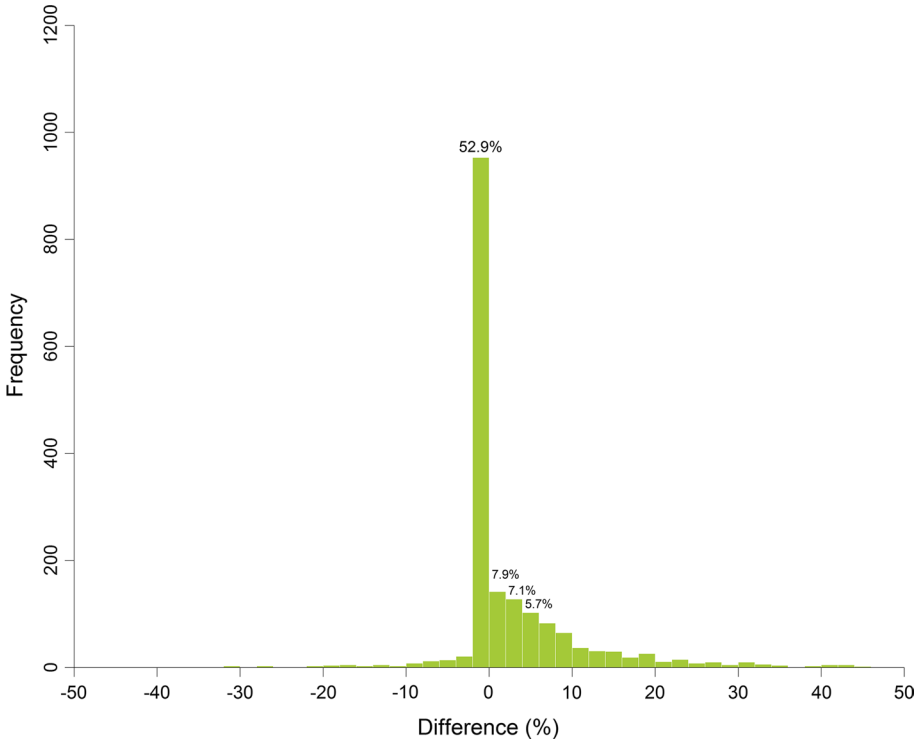

Fig. 3 Frequency histogram of difference between the simulated annual precipitation and the observed one for the baseline period. We split the differences in precipitation into 50 intervals from −50 to 50 % (each interval with a length of 2 %). The frequency of each interval is calculated as the total number of grid cells with their differences falling within the interval. The corresponding percent of each interval is calculated and only those intervals with percent greater than 5 % are labeled (*above* the *bar*)

differences varying within [0, 20] %. This may suggest that the PRECIS ensemble is likely to slightly underestimate the observed annual precipitation in the south but it tends to generate more precipitation in the north. Considering that the geographical conditions (e.g., topography and lake boundaries) of the study area may play a critical role in regulating the local precipitation (Gula and Peltier 2012), this may further indicate that the PRECIS model itself performs poor in simulating the precipitation over the regions with large bodies of water and inland seas. To further analyze the magnitude of differences in annual precipitation over all grid cells, we draw a frequency histogram of these differences (shown in Fig. 3). It can be found that the total percent of grid cells with their differences within [−2, 2] % is higher than 60 % (i.e., 52.9 % for the interval of [−2, 0] % and 7.9 % for [0, 2] %), while grid cells with differences within [2, 10] % account for at least another 20 % of the total. This confirms that the PRECIS ensemble performs very well in simulating the observed annual precipitation over Ontario.

Similarly, we further validate the performance of the PRECIS ensemble in simulating the observed seasonal precipitation over Ontario. The maps of difference in seasonal precipitation are shown in Fig. 4 and the corresponding frequency histograms are presented Fig. 5, respectively. It is interesting to find that the PRECIS ensemble is not always showing good performance in hindcasting seasonal precipitation although it is generally capable of capturing the observed annual precipitation over Ontario. In detail, the ensemble shows reasonable performance in simulating winter, summer, and autumn precipitation but its performance in spring precipitation is relatively poor (i.e., a great number of grid cells shows positive differences higher than 10 %). The frequency histogram for spring precipitation further confirms its poor performance because the grid cells with differences within [−10, 10] % only accounts for ~20 % of the total while the remaining grid cells are all showing positive differences greater than 10 %. However, the overestimation in spring precipitation appears to be offset by slight negative biases in the other seasons. In other words, the overwhelming majority of grids cells are showing negative differences within [−2, 0] % in the other seasons (i.e., 64.9 % in winter, 85.4 % in summer, and 63.4 % in autumn). The negative differences in these three seasons are likely to balance the positive bias in spring precipitation, and thus enabling the PRECIS ensemble capable of capturing the observed annual precipitation.

3.2 Projections of precipitation at major cities

Probabilistic projections of precipitation at all grid cells over Ontario in the twenty-first century are divided into three 30-year periods: 2020–2049 (or 2030 s), 2040–2069 (or 2050 s), and 2070–2099 (or 2080 s), to help understand the near-term and long-term outcomes of precipitation in the context of Ontario due to global warming. Here we first analyze future precipitation projections for 17 major cities which are geographically distributed across the landmass

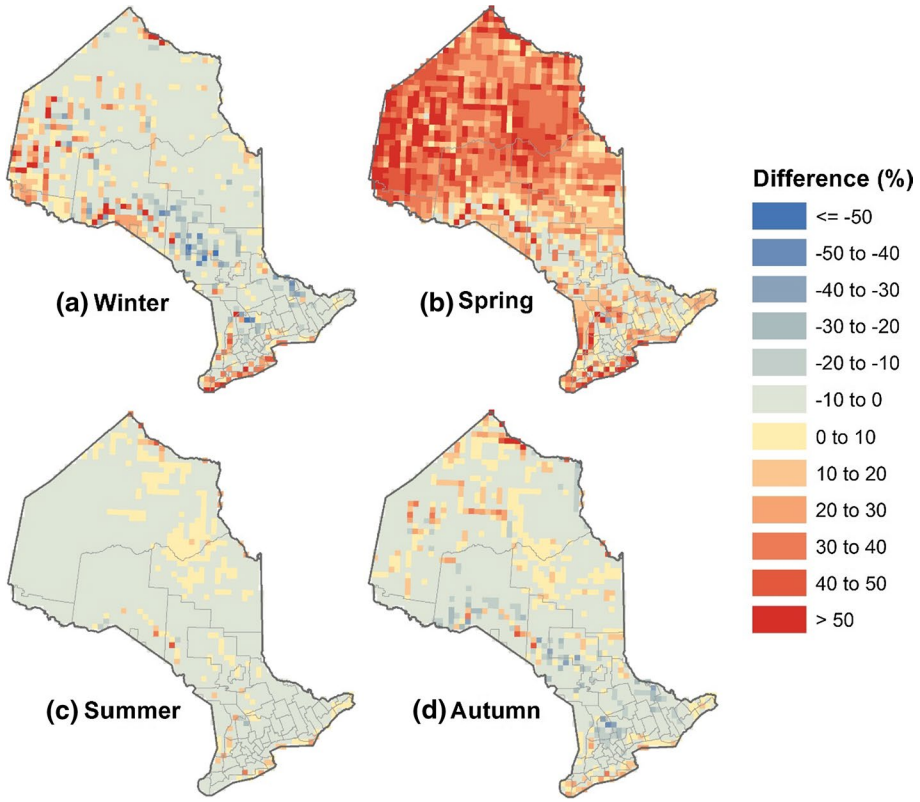

Fig. 4 Difference between the simulated seasonal precipitation and the observed one for the baseline period

of Ontario (see Fig. 1). Figure 6 shows the probability distributions of annual precipitation at these major cities in 2030, 2050, and 2080 s. Every city presents distinct probability distributions for the three periods from others. For example, the mean of probability distribution for annual precipitation in Toronto is likely to increase from ~890 mm in 2030 s to ~990 mm in 2050 s, and then would decrease significantly from 2050 to 2080 s (as low as ~860 mm); meanwhile, its spread would notably reduce in 2050 s but no apparent change is projected for 2080 s in comparison to 2030 s. Similar patterns in the mean of the distribution (i.e., increasing in 2050 s and decreasing in 2080 s) are also reported in Ottawa, Kingston, and Sandy Lake, but these cities are unlikely to suffer obvious changes in the variation of the distribution. Although it is difficult to identify a generalized pattern to summary the probability distributions at all cities, it seems that the projections in 2080 s are likely to have the highest uncertainty (represented by the widely-spread distributions at most of the stations in Fig. 6). We also generate the plots of among-member spread using the original outputs of the PRECIS ensemble simulations to help understand the uncertainties caused by different boundary conditions. Readers may refer to Figures S1, S2, and S3 in the Supplementary Material for more details.

Instead of comparing the probability distributions in annual precipitation among three future periods (i.e., 2030, 2050, and 2080 s), we calculate the central estimate of each distribution for all future periods and compare it to the observed annual precipitation in the baseline period. This is to help understand the most likely outcomes of annual precipitation in each future period and the corresponding changes relative to the baseline period. Figure 7 shows the likely trends in annual precipitation at major cities from 2030 to 2080 s relative to the baseline period. Although there is unlikely to be a continuous increase in annual precipitation from 2030 to 2080 s, we find that the vast majority of cities are likely to experience an increase in annual precipitation in three future periods in comparison to the baseline observations. For example, annual precipitation in Ottawa is projected to be 1017 mm in 2030 s and would rise up to 1084 mm in 2050 s, while in 2080 s it is likely to drop below the level in 2030 s but it is still greater than the observed precipitation in the baseline period by 8 %. Negative changes in precipitation are projected in the cities of Owen Sound and Sudbury for 2030 and 2050 s only, but their annual precipitation is likely to increase significantly in 2080 s (by 38 % in Owen Sound and 12 % in Sudbury). This may suggest that the whole province of Ontario is likely to gain more annual precipitation throughout the twenty-first century in response to global warming.

Probability distributions of seasonal precipitation at major cities for three future periods are also developed to help understand the temporal patterns in their means and variations (shown in Figs. 8, 9, 10, 11). Similar to

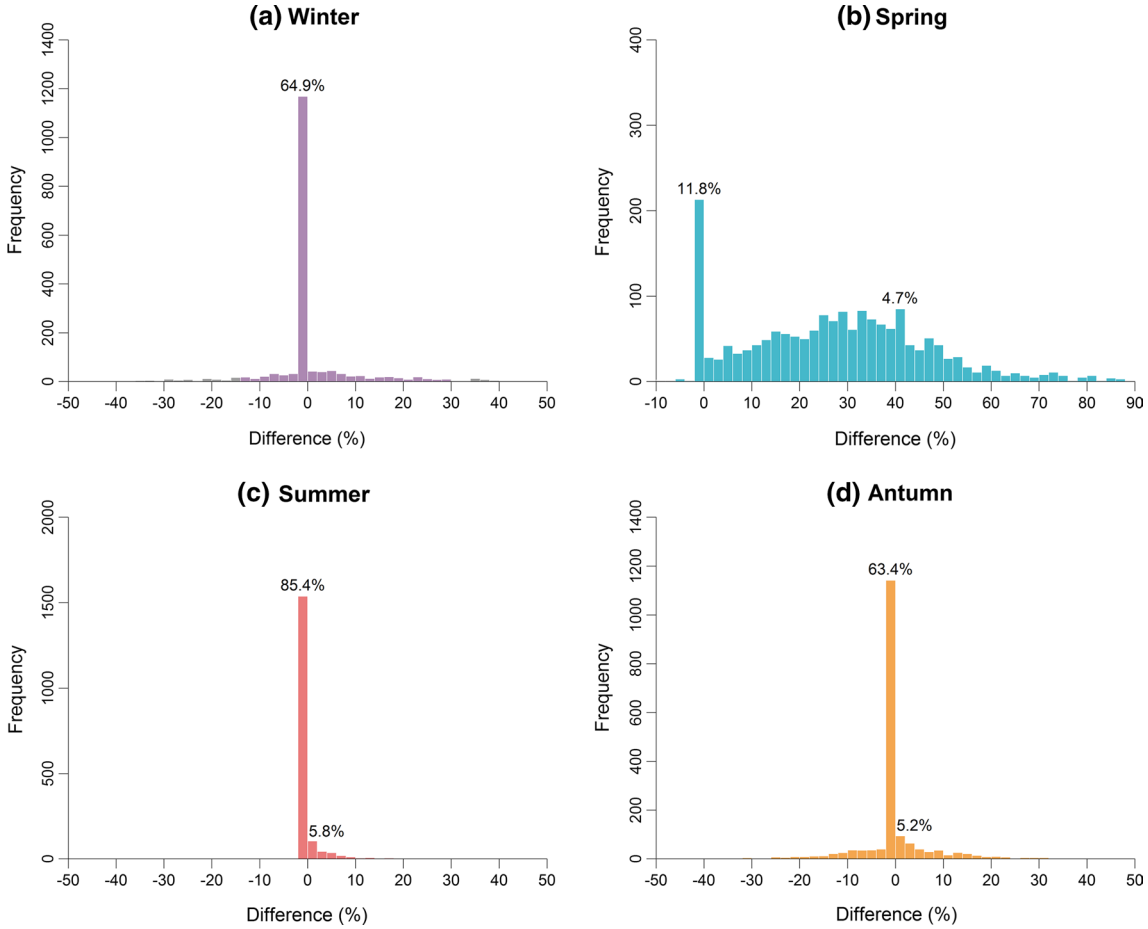

Fig. 5 Frequency histograms of difference between the simulated seasonal precipitation and the observed one for the baseline period. The differences in seasonal precipitation are split into a number of equally-wide intervals (each interval with a length of 2 %). The frequency of each interval is calculated as the total number of grid cells with their differences falling within the interval. The corresponding percent of each interval is calculated and only those intervals with percent greater than 4.5 % are labeled (*above* the *bar*)

the variability in annual precipitation distribution, each city presents distinct patterns from others in terms of the mean and variation of seasonal precipitation distribution. Furthermore, the distribution pattern in each season for one city is obviously different from its patterns in other seasons. For example, the distribution of winter precipitation in Toronto is likely to suffer a noteworthy jump in its mean from 2030 to 2050 s but only a slight increase is projected from 2050 to 2080 s; meanwhile, its variation is likely to be slightly enlarged from 2030 to 2080 s. By contrast, the distribution of summer precipitation in Toronto is projected to suffer a completely reversed pattern in its mean (i.e., a continuous decrease is reported from 2030 to 2080 s); in the meantime, its spread is likely to be slightly shrunk from 2030 to 2050 s but would be considerably widened afterwards.

To further analyze the plausible outcomes of seasonal precipitation at major cities, we calculate the central estimates in 2030, 2050, and 2080 s from their seasonal precipitation distributions and compare them with the observations in the baseline period. The results are shown in Table 1. We also calculate the percentage changes in the central estimates of seasonal and annual precipitation at major cities in 2030, 2050, and 2080 s relative to the baseline period. Table 2 shows the calculated changes for each city and the average changes for all major cities. It seems that the most significant changes in seasonal precipitation are projected in winter. For example, the winter precipitation in Toronto would be 225 mm in 2030 s, 259 mm in 2050 s, and 262 mm in 2080 s which are apparently above the average level (i.e., 173 mm) in the baseline period by 30.2, 49.6, and 51.5 %, respectively. Similarly, a large number of cities (e.g., Windsor, Moose Factory, Sandy Lake, and Fort Severn) are likely to suffer considerable increases in winter precipitation in three future periods, especially for 2080 s when the potential changes would be greater than 40 % and can be as high as

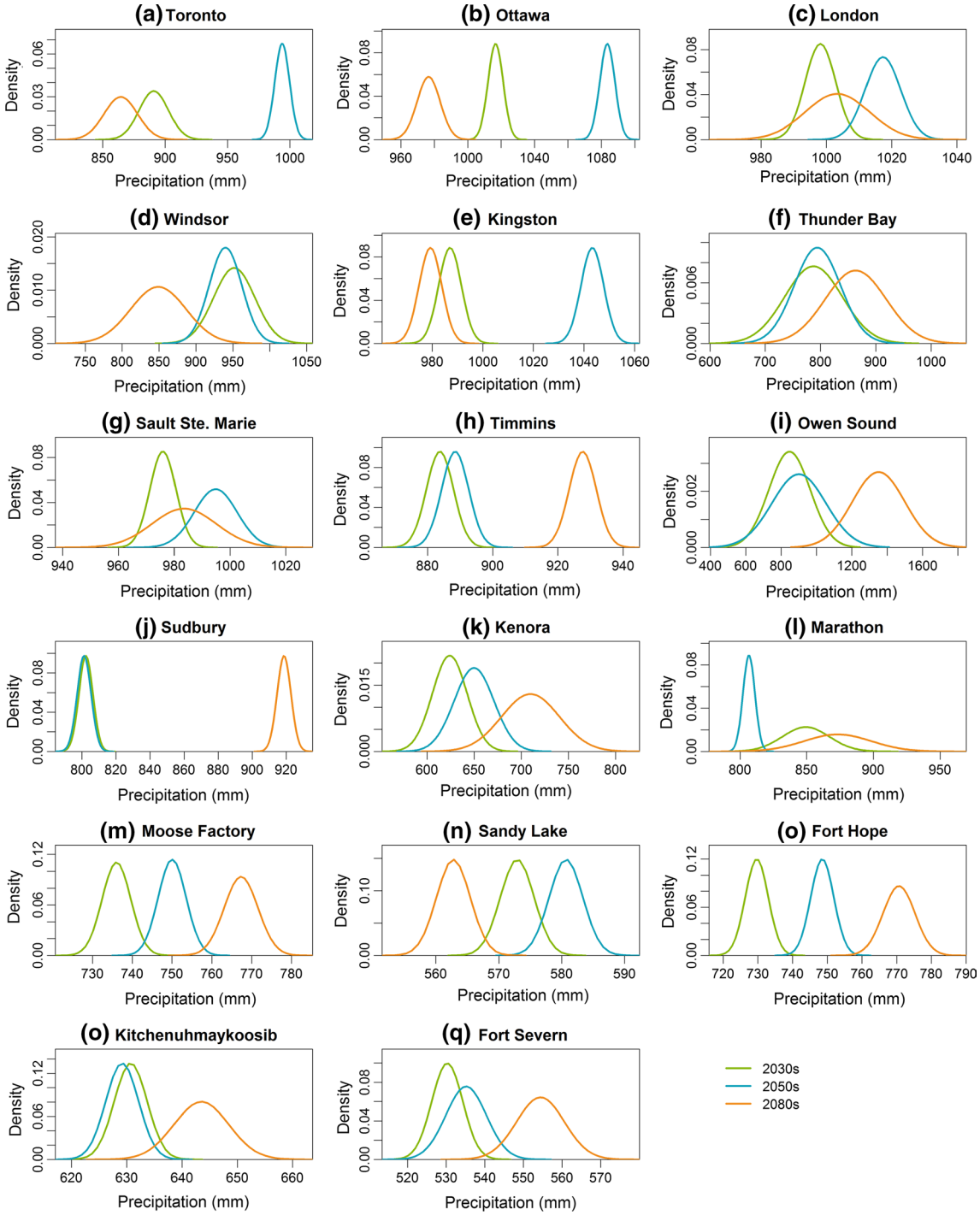

Fig. 6 Probability distributions of mean annual precipitation for future periods at major cities

62.1 %. Even though negative changes in winter precipitation are also anticipated in a few cities (e.g., Thunder Bay and Owen Sound), the average changes in winter precipitation for three future periods are still projected to increase significantly: by 11.2 % in 2030 s, 17.4 % in 2050 s, and 26.4 % in 2080 s relative to the baseline period. Likewise, the spring precipitation at most of the cities is likely to increase for three future periods, leading to an average change of 7.8 % in 2030 s, and 15.8 % in 2050 s, and 9.3 % in 2080 s. However, the summer precipitation at these cities is likely to decrease by 7.7 % on average to the end of this century although a slight increase (by 4.5 % on

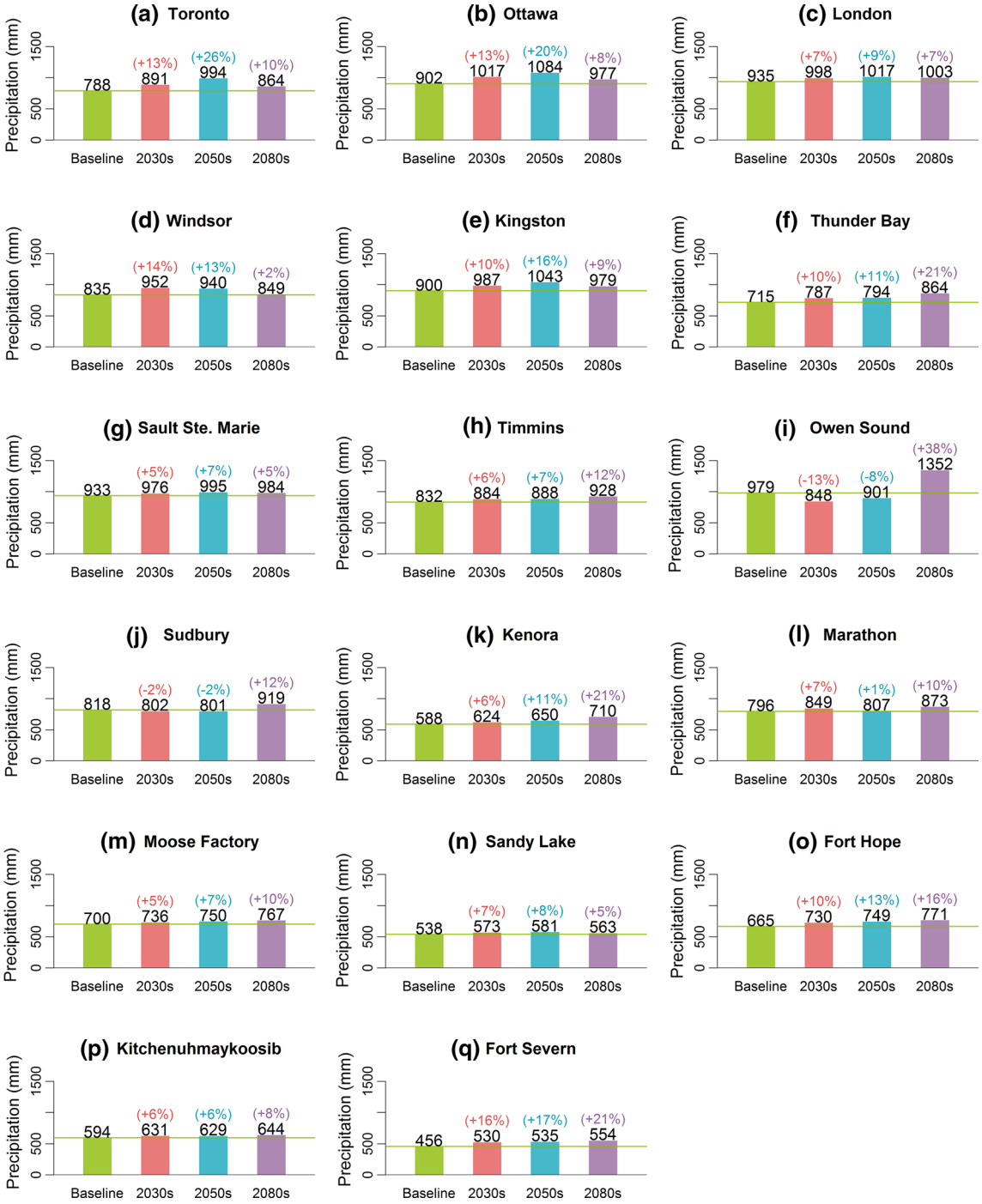

Fig. 7 Likely changes in and plausible outcomes of mean annual precipitation for future periods at major cities. Note that the values for three future periods (i.e., 2030, 2050, and 2080 s) are the central estimates (i.e., at 50 % probability) of their probabilistic projections. The values in *parentheses* indicate percentage changes in precipitation for three future periods relative to the baseline period. The sign of "+" means increase and "−" indicates decrease in annual precipitation, respectively

average) is projected in the next few decades. It seems that the majority of these cities would receive more precipitation in autumn (by 10.2 % on average) in the long run till to the end of this century, while the magnitude of changes in 2030 and 2050 s is very small on average (by -0.7 % and 1.6 %, respectively). As the selected cities in this study are largely evenly distributed within the Province of Ontario, it is reasonable to speculate that similar changes in seasonal

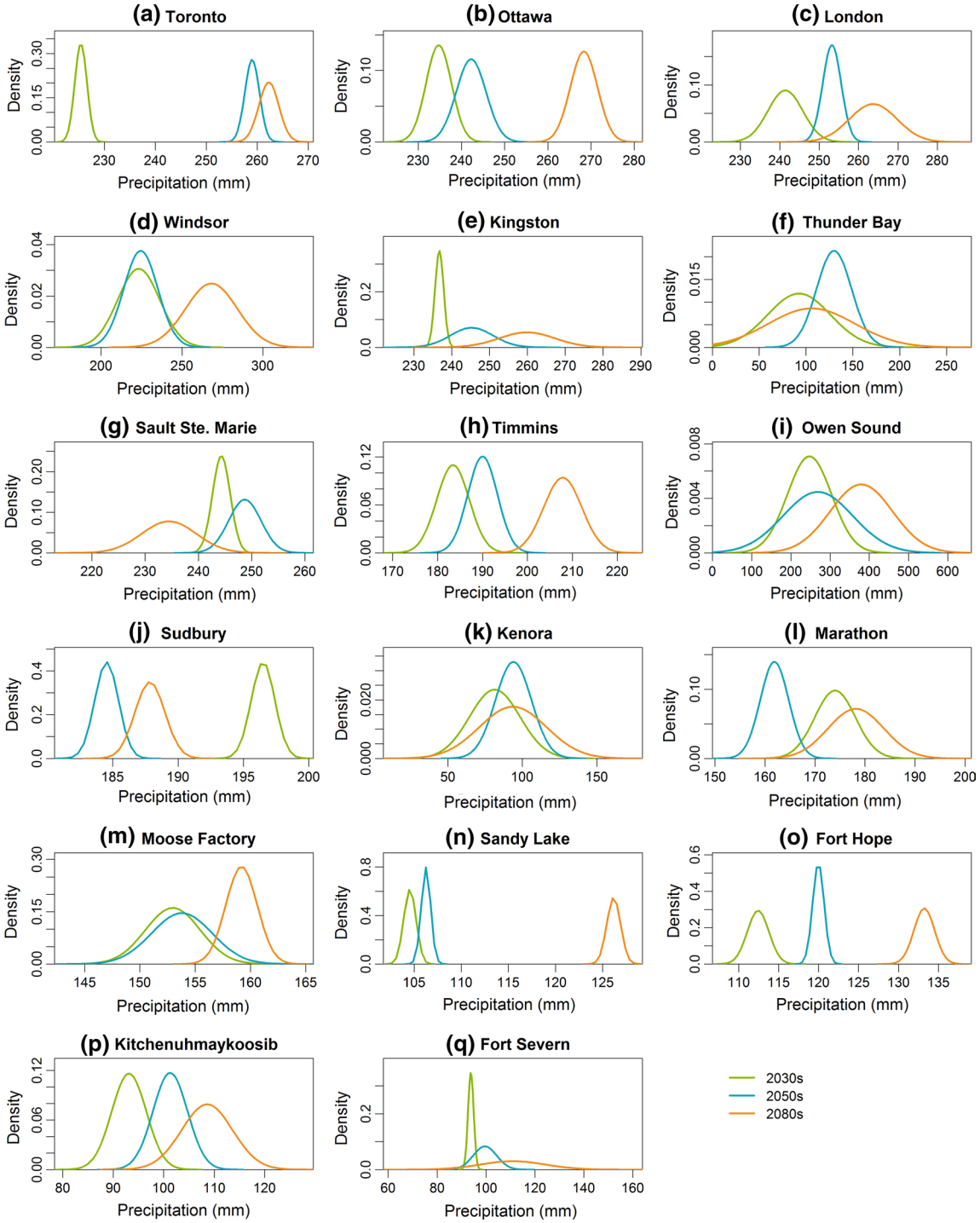

Fig. 8 Probability distribution of mean winter precipitation in 2030, 2050, and 2080 s

precipitation are likely to be anticipated for the entire province. In other words, the whole province is likely to receive more precipitation in winter, spring, and autumn throughout this century while summer precipitation tends to slightly increase in 2030 s but would decrease gradually afterwards. However, because the magnitude of projected decrease in summer precipitation is relatively small in comparison with the anticipated increases in other three seasons, the annual precipitation over the entire province is likely to suffer a progressive increase throughout this century (by 7.0 % in 2030 s, 9.5 % in 2050 s, and 12.6 % in 2080 s). Generally speaking, the mechanism behind the

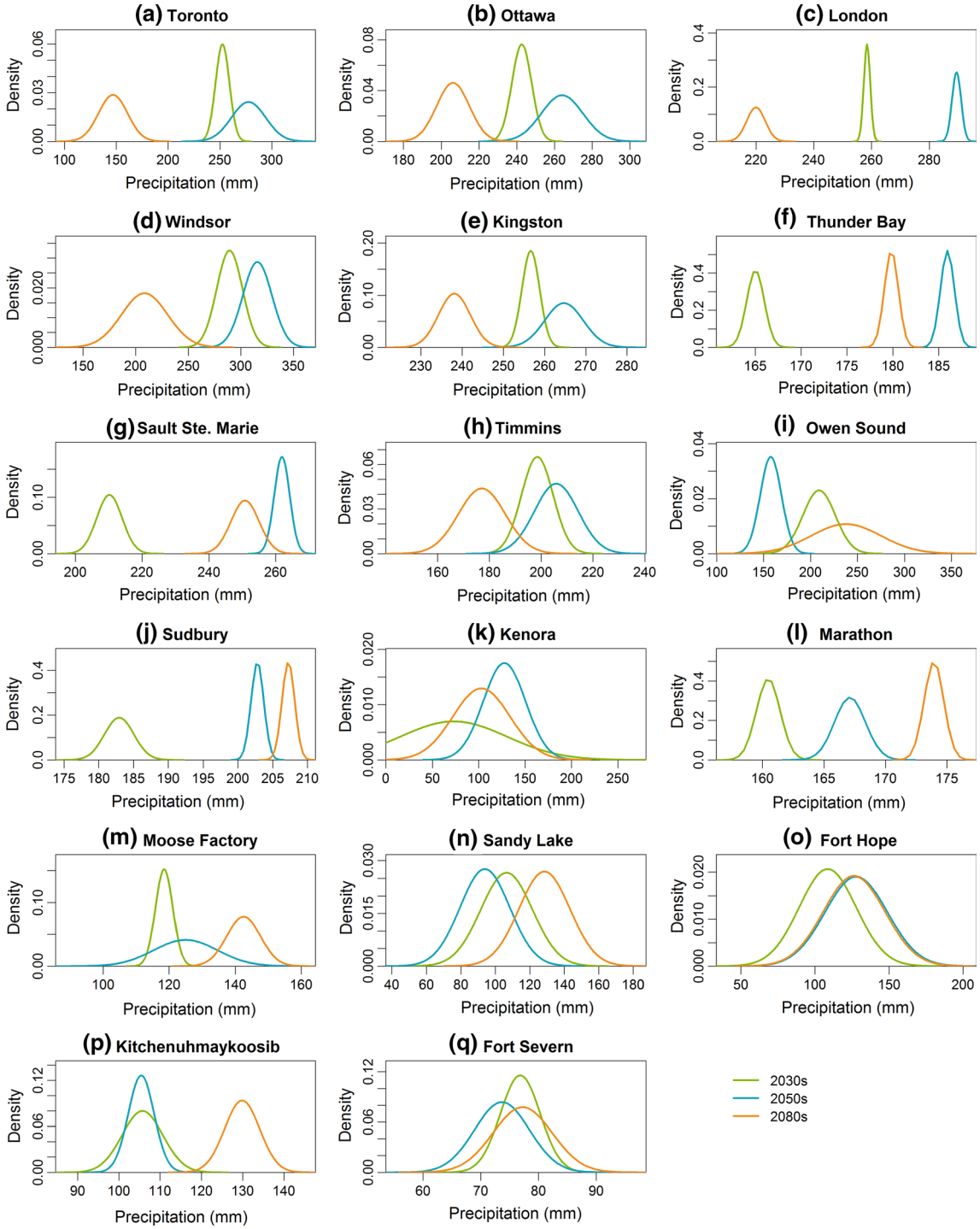

Fig. 9 Probability distribution of mean spring precipitation in 2030, 2050, and 2080 s

projected increases in precipitation is that warming temperature would lead to more evaporation and intensify the water cycle at regional scales, and thus result in more precipitation. This mechanism has already been examined and reported in many literatures (e.g., Seager et al. 2012; Stocker et al. 2014; Trenberth 2011; Wentz et al. 2007). Such a mechanism is particularly true for the Province of Ontario which is next to the Great Lakes in the south and to the Hudson Bay in the north (as shown in Fig. 1). These large bodies of water apparently play important roles in regulating the precipitation pattern over Ontario (Gula and Peltier 2012).

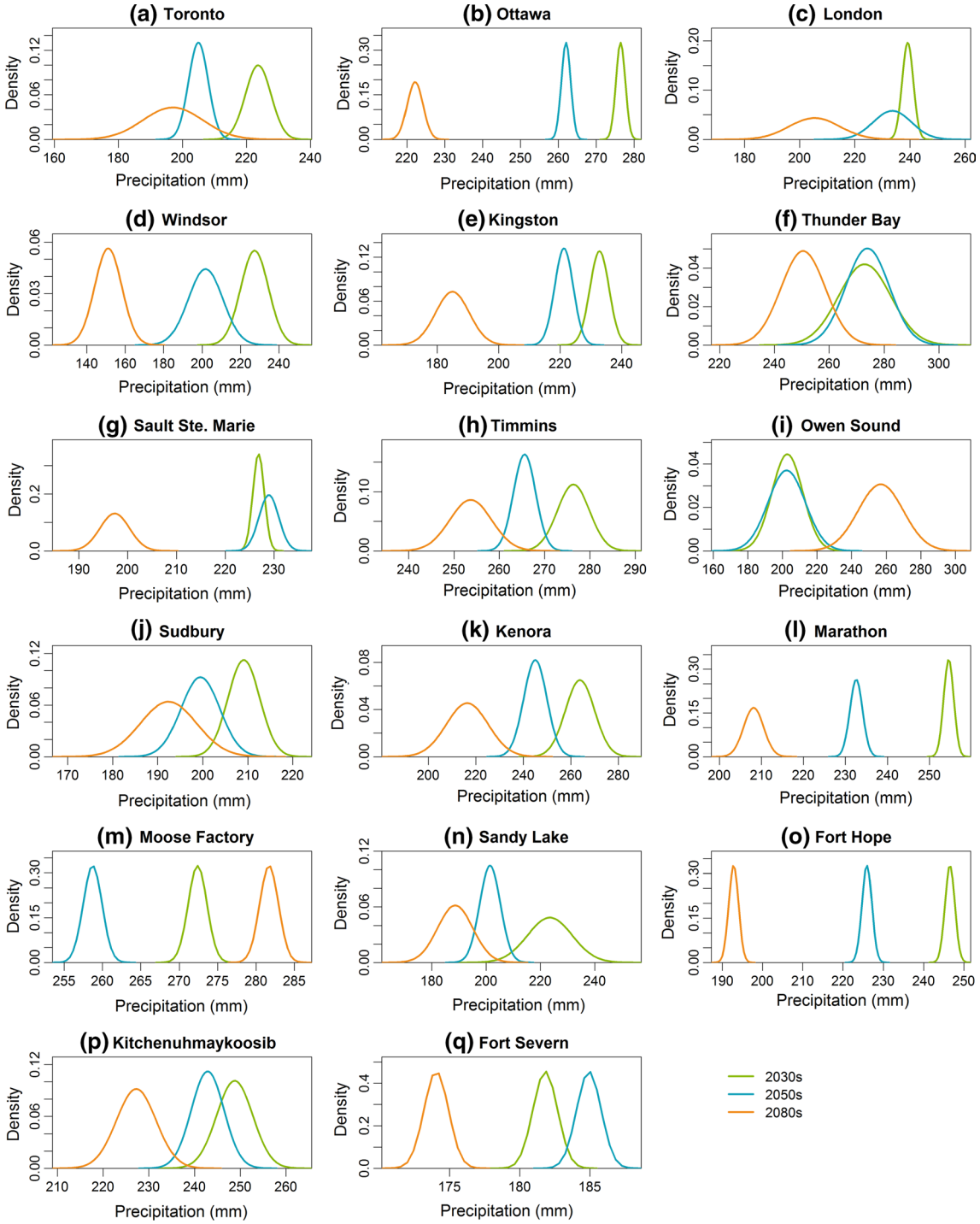

Fig. 10 Probability distribution of mean summer precipitation in 2030, 2050, and 2080 s

3.3 Projections of precipitation over Ontario

Following the analyses on precipitation projections at major cities, here we present the developed probabilistic projections for the Province of Ontario. Figure 12 shows the projections of annual precipitation for three future periods at three typical probability levels (i.e., 10, 50, and 90 %). There is an apparent gradually increasing pattern along with the latitude for annual precipitation. For example, the central estimates of annual precipitation in the north is projected to be mostly varying within [500, 700] mm in 2030 s, while in the middle and the south the medians of

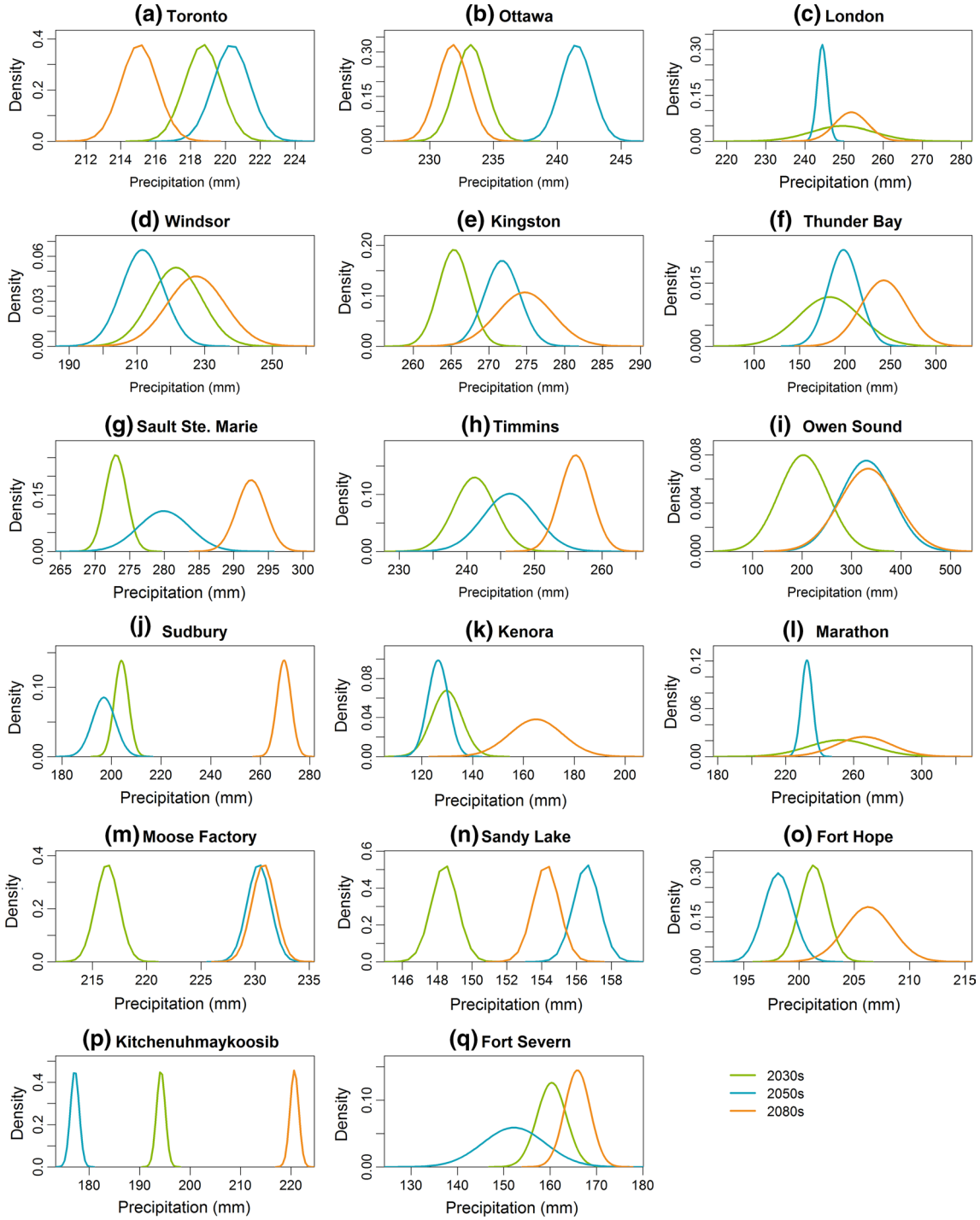

Fig. 11 Probability distribution of mean autumn precipitation in 2030, 2050, and 2080 s

annual precipitations in the same period would largely be [700, 900] mm and [900, 1100] mm, respectively. Besides, it appears that such a meridionally distributed pattern in annual precipitation across the entire province is unlikely to change too much in 2050 and 2080 s, although evident spatial variations in annual precipitation are still projected at local scales (e.g., in the south end). As for the temporal trend in annual precipitation, it is clear that the whole province of Ontario would suffer a continuous increase in its annual precipitation from 2030 to 2080 s because the areas with annual precipitation less than 600 mm are gradually reduced after 2030 s. However, we should note that slight

Table 1 Comparison between the central estimates of seasonal precipitation at major cities in 2030, 2050, and 2080 s and the observations in the baseline period

No.	City	Winter				Spring				Summer				Autumn			
		Baseline	2030 s	2050 s	2080 s	Baseline	2030 s	2050 s	2080 s	Baseline	2030 s	2050 s	2080 s	Baseline	2030 s	2050 s	2080 s
1	Toronto	173	225	259	262	192	252	278	147	211	224	205	197	210	219	220	215
2	Ottawa	206	235	242	268	205	243	264	206	245	276	262	222	246	233	241	232
3	London	224	241	253	264	223	258	289	220	236	239	234	205	252	250	244	252
4	Windsor	178	223	225	268	214	289	316	209	237	227	202	151	204	222	212	228
5	Kingston	229	237	245	260	215	257	265	238	200	233	221	185	258	265	272	275
6	Thunder Bay	122	93	130	106	153	165	186	180	246	273	274	251	195	183	198	243
7	Sault Ste. Marie	229	244	249	234	195	210	262	251	234	227	229	197	277	273	280	293
8	Timmins	164	183	190	208	171	198	206	177	267	276	266	254	231	241	246	256
9	Owen Sound	283	248	269	380	193	209	158	238	226	203	203	257	278	203	330	334
10	Sudbury	181	196	185	188	182	183	203	207	213	209	199	192	243	204	197	270
11	Kenora	80	81	94	94	116	73	128	103	248	264	245	216	144	130	126	165
12	Marathon	165	174	162	178	158	160	167	174	239	255	233	208	236	252	232	266
13	Moose Factory	113	153	154	159	124	118	125	143	246	272	259	282	216	216	230	231
14	Sandy Lake	84	105	106	126	95	106	94	128	208	223	201	189	151	148	157	154
15	Fort Hope	104	112	120	133	123	109	128	126	244	247	226	193	193	201	198	206
16	Kitchenuhmaykoosib	88	93	101	109	101	106	105	130	232	249	243	227	174	194	177	221
17	Fort severn	68	94	100	111	73	77	74	77	174	182	185	174	141	160	152	166

Table 2 Changes in the central estimates of seasonal and annual precipitation at major cities in 2030, 2050, and 2080 s (relative to the baseline period)

No.	City name	Winter			Spring			Summer			Autumn			Annual		
		2030 s (%)	2050 s (%)	2080 s (%)	2030 s (%)	2050 s (%)	2080 s (%)	2030 s (%)	2050 s (%)	2080 s (%)	2030 s (%)	2050 s (%)	2080 s (%)	2030 s (%)	2050 s (%)	2080 s (%)
1	Toronto	30.2	49.6	51.5	31.5	44.7	−23.4	5.8	−3.0	−6.8	4.0	4.8	2.3	13.1	26.2	9.7
2	Ottawa	13.8	17.4	30.0	18.4	28.9	0.6	12.6	6.8	−9.5	−5.2	−1.8	−5.7	12.8	20.2	8.3
3	London	7.6	12.9	17.5	16.1	30.0	−1.2	1.3	−1.0	−13.0	−1.1	−3.1	−0.2	6.8	8.8	7.3
4	Windsor	25.2	25.9	50.4	35.0	47.4	−2.7	−4.2	−14.9	−36.3	8.5	3.6	11.3	14.0	12.6	1.7
5	Kingston	3.5	7.2	13.6	19.2	22.9	10.6	16.7	10.9	−7.3	3.0	5.4	6.6	9.6	15.9	8.8
6	Thunder Bay	−23.8	6.8	−12.8	7.9	21.6	17.6	11.0	11.4	1.9	−6.4	1.6	24.2	10.1	11.0	20.7
7	Sault Ste. Marie	6.9	8.8	2.6	8.1	34.6	28.9	−3.1	−2.2	−15.7	−1.6	0.9	5.4	4.6	6.6	5.4
8	Timmins	12.1	16.1	27.0	16.2	20.5	3.6	3.6	−0.4	−4.9	4.5	6.7	10.9	6.2	6.8	11.5
9	Owen Sound	−12.7	−5.0	33.9	8.2	−18.4	23.1	−10.1	−10.2	13.9	−27.1	18.8	20.1	−13.4	−7.9	38.1
10	Sudbury	8.8	2.2	4.0	0.4	11.3	13.7	−1.9	−6.4	−9.8	−16.0	−18.9	11.0	−1.9	−2.0	12.4
11	Kenora	2.3	18.0	17.6	−37.2	9.6	−11.6	6.4	−1.2	−12.7	−9.7	−12.1	14.7	6.2	10.6	20.8
12	Marathon	5.4	−2.0	7.9	1.6	5.8	10.1	6.7	−2.5	−12.8	7.1	−1.4	12.9	6.7	1.3	9.7
13	Moose Factory	35.4	36.2	40.9	−4.3	0.9	15.1	10.5	5.0	14.3	−0.1	6.4	6.6	5.1	7.1	9.6
14	Sandy Lake	24.3	26.3	50.0	12.2	−1.1	35.3	7.6	−3.0	−9.2	−1.7	3.8	2.2	6.5	7.9	4.6
15	Fort Hope	7.8	15.0	27.7	−11.7	3.9	2.7	1.1	−7.4	−20.9	4.4	2.8	7.0	9.7	12.6	15.9
16	Kitchenuh-maykoosib	6.3	15.6	24.0	5.0	4.7	29.0	7.4	4.8	−1.9	11.5	1.7	26.7	6.1	5.9	8.3
17	Fort Severn	37.0	45.5	62.1	5.5	1.2	6.1	4.3	6.1	−0.1	14.1	8.3	18.1	16.2	17.3	21.5
	Average	11.2	17.4	26.4	7.8	15.8	9.3	4.5	−0.4	−7.7	−0.7	1.6	10.2	7.0	9.5	12.6

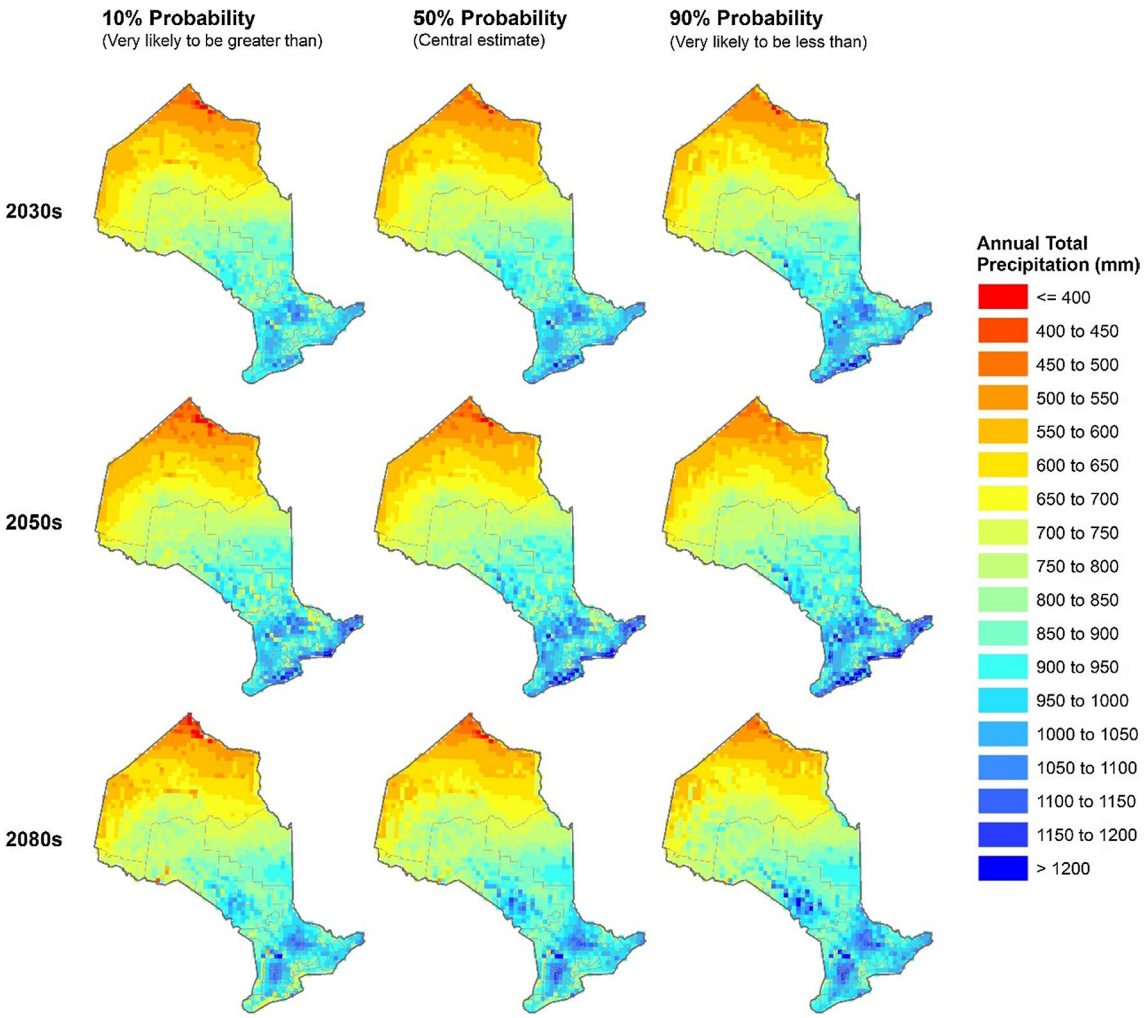

Fig. 12 Projections of mean annual precipitation over Ontario in 2030, 2050, and 2080 s

decreases are also likely to occur in some southern regions with their annual precipitation greater than 1000 mm.

Figure 13 shows the central estimates of seasonal precipitation over Ontario for three future periods, while Fig. 14 presents the frequency histograms of seasonal precipitation in future periods for all grid cells within the domain of Ontario. Similar meridionally-increasing patterns in seasonal precipitation (i.e., less in the north and more in the south) are also projected for winter, spring, and autumn, apart from summer when no obvious spatial pattern is reported. Besides, there are clear temporally-increasing trends throughout this century for winter, spring, and autumn precipitation. For example, in the north, the areas with winter precipitation less than 110 mm or spring precipitation less than 90 mm are apparently reduced from 2030 to 2080 s; while the southern areas with autumn precipitation greater than 270 mm are evidently increased. We also notice that there is likely to be a sharp increase in spring precipitation from [210, 290] mm in 2030 s to [250, 330] mm in 2050 s in most areas of south Ontario but afterwards it would drop to [190, 250] mm in 2080 s. By contrast, the central estimates of summer precipitation over Ontario are likely to decrease slightly from 2030 to 2080 s. This is especially true in the middle-west where summer precipitation would decline gradually from [250, 290] mm in 2030 s to [230, 270] mm in 2080 s. However, the projected decrease in summer precipitation is unlikely to offset the evident increases in other three seasons which consequently lead to an overall increasing trend in annual precipitation over Ontario throughout the twenty-first century.

To further investigate the uncertainties involved in the probabilistic projections of precipitation in the context

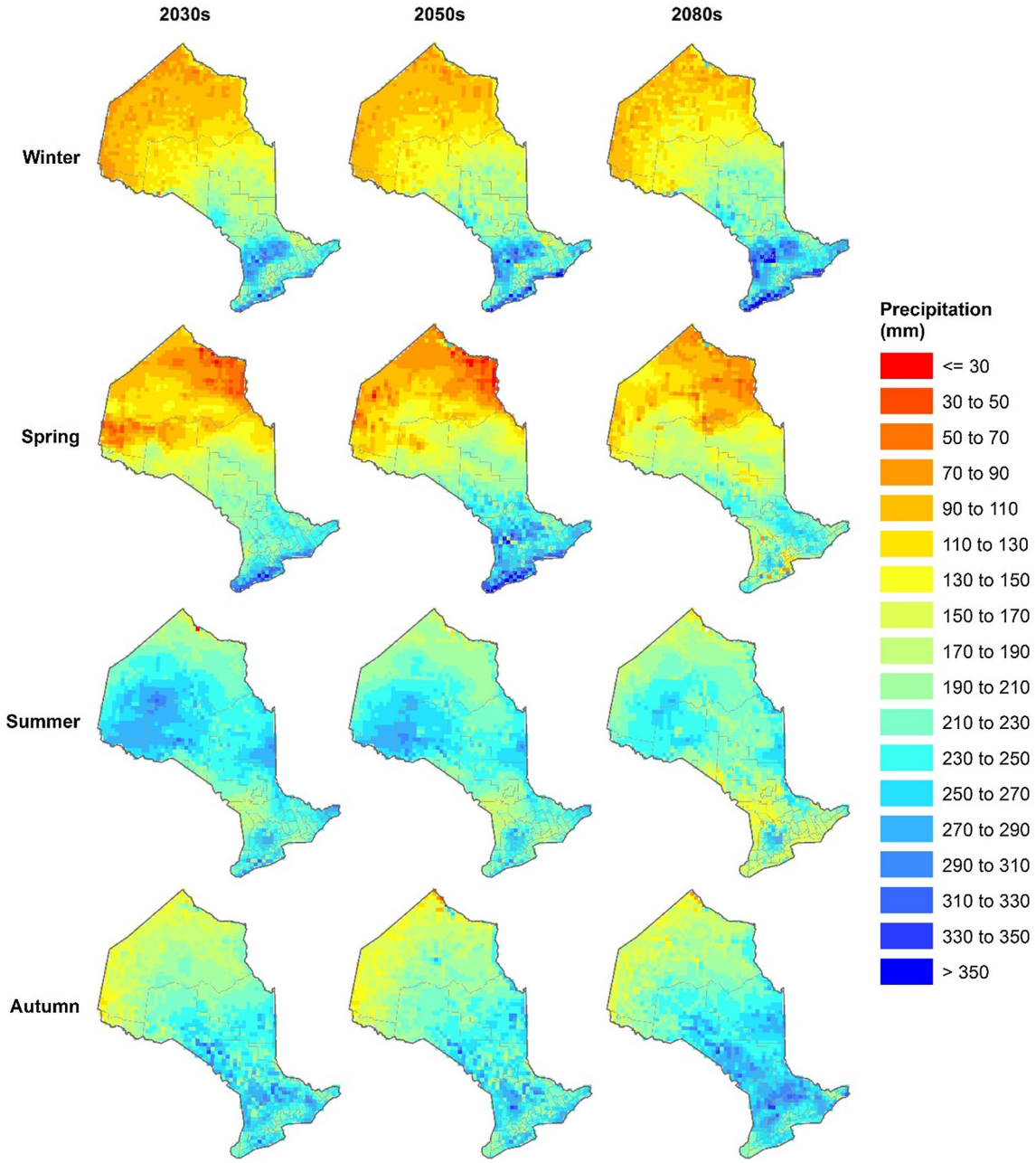

Fig. 13 Projections of seasonal precipitation over Ontario in 2030, 2050, and 2080 s (50 % probability)

of Ontario, we here introduce the degree of uncertainty which is defined as the width or spread of the most likely range bounded by the estimates at 10 and 90 % probability. The unit of the degree of uncertainty is mm. Accordingly, the wider the range is, the more uncertain or the less reliable the projections are. Figure 15 shows the maps of degree of uncertainty for annual and seasonal precipitation for three future periods. For the seasonal precipitation, we notice that the projections for winter, summer, and autumn present relatively small degrees of uncertainty (mostly ranging within [0, 10] mm) while the spring projections manifest high degrees of uncertainty which may vary between 0 and 50 mm. This is especially true in the middle-west where the degree of uncertainty for spring precipitation would be as high as [25, 50] mm. This may suggest that the projections for spring precipitation obtained through the PRECIS ensemble are less reliable than those for the other three

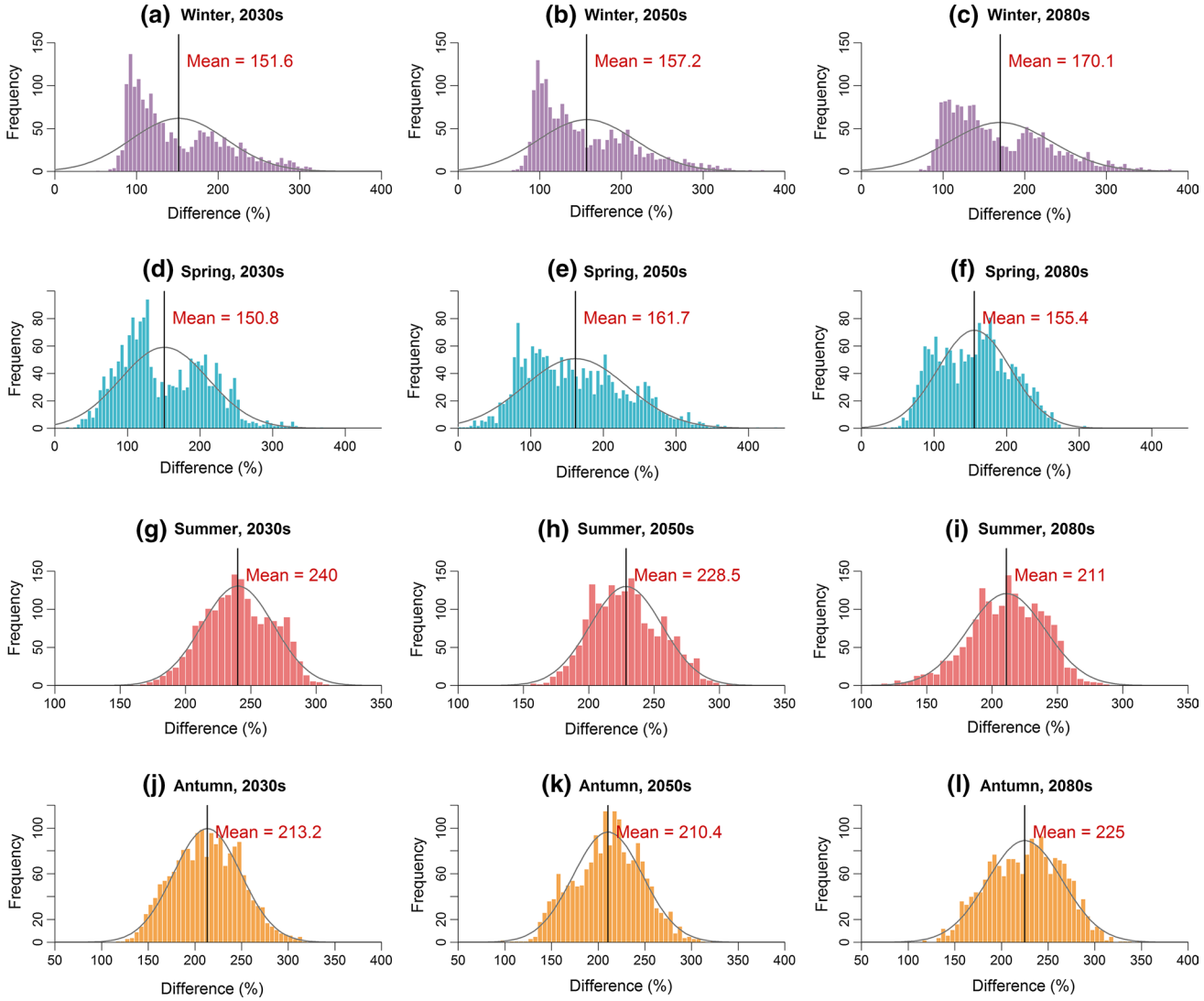

Fig. 14 Frequency histograms of seasonal precipitation for all grid cells in 2030, 2050, and 2080 s (50 % probability)

seasons. Consequently, this will further result in more uncertainties in annual precipitation projections whose degrees of uncertainty are mainly varying between 0 and 20 mm.

4 Conclusions

In this study, high-resolution probabilistic projections of precipitation were developed for the Province of Ontario with the purpose of investigating how global warming would affect the local precipitation at major cities and across the entire province. We first performed five-member RCM ensemble simulations using the PRECIS regional climate modeling system. The PRECIS ensemble simulations were driven by a set of boundary conditions from a HadCM3-based perturbed-physics ensemble under A1B emission scenario. Changes in precipitation projected by each member of the ensemble were then calculated and fed into a Bayesian hierarchical model to generate probabilistic precipitation changes at 25 km grid point scales. Following that, we developed reliable precipitation projections throughout the twenty-first century for the entire province by applying the probabilistic changes to the observed precipitation.

Simulations of annual and seasonal precipitation for the baseline period were compared to the observations to validate the capability of the PRECIS ensemble in capturing the spatial patterns of precipitation over Ontario. The validation results showed that the PRECIS ensemble performs very well in simulating the observed annual precipitation and seasonal precipitation in winter, summer, and autumn

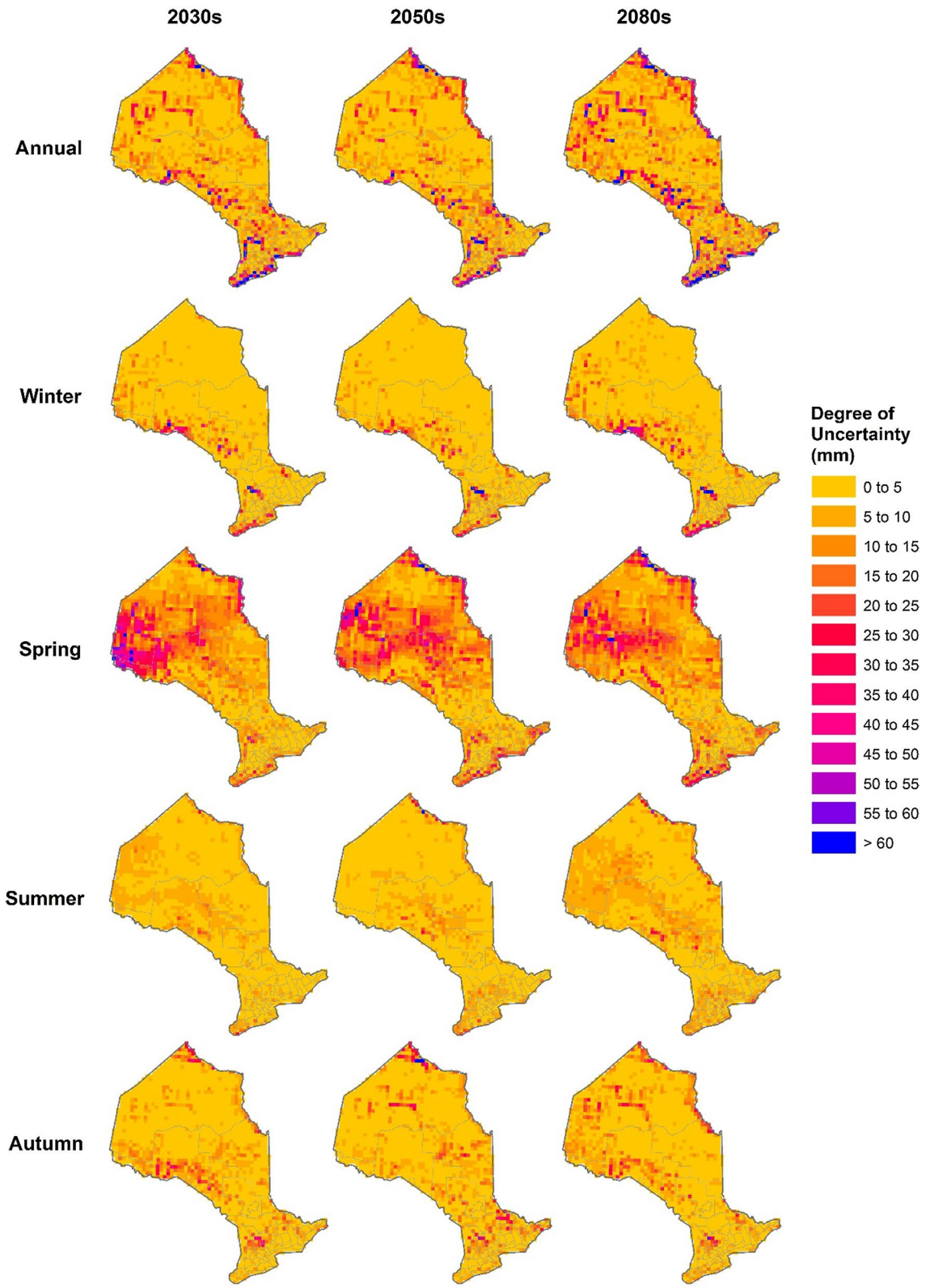

Fig. 15 Maps of degree of uncertainty for annual and seasonal precipitation projections

while its performance in hindcasting spring precipitation is relatively poor. The ensemble simulations were then synthesized through a Bayesian hierarchical model to develop probabilistic projections of precipitation with consideration of some uncertain parameters involved in the regional climate modeling process. The results showed that the vast majority of cities are likely to gain positive changes in annual precipitation in 2030, 2050, and 2080 s in comparison to the observations in the baseline period. This may suggest that the whole province of Ontario is likely to receive more annual precipitation throughout the twenty-first century in response to global warming. Our analyses on the projections of seasonal precipitation further showed that the entire province is likely to receive more precipitation in winter, spring, and autumn throughout this century while summer precipitation is only likely to increase slightly in 2030 s but would decrease gradually afterwards. However, because the magnitude of projected decreases in summer precipitation is relatively small in comparison with the anticipated increases in other three seasons, the annual precipitation over Ontario is likely to suffer a progressive increase throughout the twenty-first century (by 7.0 % in 2030 s, 9.5 % in 2050 s, and 12.6 % in 2080 s). The degree of uncertainty for precipitation projections was also analyzed in this study. The results suggest that future changes in spring precipitation show higher degree of uncertainty than other seasons, resulting in more uncertainties in annual precipitation projections.

It is interesting to find that the PRECIS model performs poorly in simulating spring precipitation over Ontario while it does show good performance in capturing precipitation of other three seasons. Considering that the observed spring temperature of Ontario is usually floating up or down around 0 °C (see Figure S4 in the Supplementary Material) while temperature in other three seasons is either lower than 0 °C (i.e., winter) or greater than 0 °C (i.e., summer and autumn), the possible reasons behind the apparent bias in spring precipitation might be: (1) the PRECIS model cannot well determine the phase of the precipitation (i.e., snowfall or rainfall) while temperature is fluctuating around 0 °C; (2) the PRECIS model cannot well simulate the physics of frozen soil (or permafrost) in northern Ontario (Tam 2009) when temperature is fluctuating around 0 °C. However, these are not necessarily the real reasons because there are many physical processes and/or parameters may directly or indirectly affect the simulated precipitation. Future research efforts through sensitivity experiments are still required to investigate the real causes behind poor performance in spring precipitation. Here we should note that to minimize the effects of the modeling bias on the reliability of future precipitation projections, we only used the ensemble simulations to calculate the percentage changes in precipitation. Future precipitation projections were developed by applying the projected changes to the observed precipitation for the current climate of Ontario. In this sense, the developed probabilistic precipitation projections in this study were bias-corrected and thus can provide helpful information for assessing the potential effects of climate change in the context of Ontario.

Acknowledgments This research was supported by the Natural Sciences Foundation (51190095, 51225904), the Program for Innovative Research Team in University (IRT1127), Ontario Ministry of the Environment and Climate Change, and the Natural Science and Engineering Research Council of Canada.

References

Abatzoglou JT, Brown TJ (2012) A comparison of statistical downscaling methods suited for wildfire applications. Int J Climatol 32(5):772–780

Akhtar M, Ahmad N, Booij M (2008) The impact of climate change on the water resources of Hindukush–Karakorum–Himalaya region under different glacier coverage scenarios. J Hydrol 355(1):148–163

Aldous A, Fitzsimons J, Richter B, Bach L (2011) Droughts, floods and freshwater ecosystems: evaluating climate change impacts and developing adaptation strategies. Mar Freshw Res 62(3):223–231

Allan RP, Soden BJ (2008) Atmospheric warming and the amplification of precipitation extremes. Science 321(5895):1481–1484

Bárdossy A, Pegram G (2013) Interpolation of precipitation under topographic influence at different time scales. Water Resour Res 49(8):4545–4565

Barnett DN, Brown SJ, Murphy JM, Sexton DM, Webb MJ (2006) Quantifying uncertainty in changes in extreme event frequency in response to doubled CO2 using a large ensemble of GCM simulations. Clim Dyn 26(5):489–511

Baron J, Hall E, Nolan B, Finlay J, Bernhardt E, Harrison J, Chan F, Boyer E (2013) The interactive effects of excess reactive nitrogen and climate change on aquatic ecosystems and water resources of the United States. Biogeochemistry 114(1–3):71–92

Chou C, Neelin JD, Chen C-A, Tu J-Y (2009) Evaluating the "rich-get-richer" mechanism in tropical precipitation change under global warming. J Clim 22(8):1982–2005

Christensen NS, Lettenmaier DP (2007) A multimodel ensemble approach to assessment of climate change impacts on the hydrology and water resources of the Colorado River Basin. Hydrol Earth Syst Sci 11(4):1417–1434

Collins M, Booth BB, Harris GR, Murphy JM, Sexton DM, Webb MJ (2006) Towards quantifying uncertainty in transient climate change. Clim Dyn 27(2–3):127–147

Cross MS, Zavaleta ES, Bachelet D, Brooks ML, Enquist CA, Fleishman E, Graumlich LJ, Groves CR, Hannah L, Hansen L (2012) The Adaptation for Conservation Targets (ACT) framework: a tool for incorporating climate change into natural resource management. Environ Manage 50(3):341–351

Dai A (2011) Drought under global warming: a review. Wiley Interdiscip Rev Clim Change 2(1):45–65

Estrada F, Guerrero VM, Gay-García C, Martínez-López B (2013) A cautionary note on automated statistical downscaling methods for climate change. Clim Change 120(1–2):263–276

Feddersen H, Andersen U (2005) A method for statistical downscaling of seasonal ensemble predictions. Tellus A 57(3):398–408

Feser F, Rockel B, von Storch H, Winterfeldt J, Zahn M (2011) Regional climate models add value to global model data: a review and selected examples. Bull Am Meteorol Soc 92(9):1181–1192

Ford JD, Berrang-Ford L, Paterson J (2011) A systematic review of observed climate change adaptation in developed nations. Clim Change 106(2):327–336

Fowler A, Hennessy K (1995) Potential impacts of global warming on the frequency and magnitude of heavy precipitation. Nat Hazards 11(3):283–303

Giorgi F, Mearns LO (2002) Calculation of average, uncertainty range, and reliability of regional climate changes from AOGCM simulations via the "reliability ensemble averaging"(REA) method. J Clim 15(10):1141–1158

Giorgi F, Mearns L (2003) Probability of regional climate change based on the Reliability Ensemble Averaging (REA) method. Geophys Res Lett 30(12):1629. doi:10.1029/2003GL017130

Grafton RQ, Pittock J, Davis R, Williams J, Fu G, Warburton M, Udall B, McKenzie R, Yu X, Che N (2013) Global insights into water resources, climate change and governance. Nat Clim Change 3(4):315–321

Gula J, Peltier WR (2012) Dynamical downscaling over the Great Lakes basin of North America using the WRF regional climate model: the impact of the Great Lakes system on regional greenhouse warming. J Clim 25(21):7723–7742

He J, Valeo C, Chu A, Neumann NF (2011) Stormwater quantity and quality response to climate change using artificial neural networks. Hydrol Process 25(8):1298–1312

Heinrich G, Gobiet A, Mendlik T (2014) Extended regional climate model projections for Europe until the mid-twentyfirst century: combining ENSEMBLES and CMIP3. Clim Dyn 42(1–2):521–535

Hewitson B, Crane R (1996) Climate downscaling: techniques and application. Clim Res 7(2):85–95

Hirabayashi Y, Mahendran R, Koirala S, Konoshima L, Yamazaki D, Watanabe S, Kim H, Kanae S (2013) Global flood risk under climate change. Nat Clim Change 3(9):816–821

Hoffmann AA, Sgrò CM (2011) Climate change and evolutionary adaptation. Nature 470(7335):479–485

Hulme M, Osborn TJ, Johns TC (1998) Precipitation sensitivity to global warming: comparison of observations with HadCM2 simulations. Geophys Res Lett 25(17):3379–3382

IPCC (2014) Climate change 2014: synthesis report, summary for policymakers. Intergovernmental Panel on Climate Change

Jones RG, Noguer M, Hassell DC, Hudson D, Wilson SS, Jenkins GJ, Mitchell JFB (2004) Generating high resolution climate change scenarios using PRECIS. Met Office Handbook, Exeter, Devon

Jordan YC, Ghulam A, Chu ML (2014) Assessing the impacts of future urban development patterns and climate changes on total suspended sediment loading in surface waters using geoinformatics. J Environ Informat 24(2):65–79

Korhonen N, Venäläinen A, Seppä H, Järvinen H (2014) Statistical downscaling of a climate simulation of the last glacial cycle: temperature and precipitation over Northern Europe. Clim Past 10(4):1489–1500

Larsen MAD, Refsgaard JC, Drews M, Butts MB, Jensen KH, Christensen J, Christensen O (2014) Results from a full coupling of the HIRHAM regional climate model and the MIKE SHE hydrological model for a Danish catchment. Hydrol Earth Syst Sci 18(11):4733–4749

Ling J, Wu ML, Chen YF, Zhang YY, Dong JD (2014) Identification of spatial and temporal patterns of coastal waters in Sanya Bay, South China Sea by Chemometrics. J Environ Informat 23(1):37–43

Ma ZZ, Wang ZJ, Xia T, Gippel CJ, Speed R (2014) Hydrograph-based hydrologic alteration assessment and its application to the yellow river. J Environ Informat 23(1):1–13

Marengo JA, Alves LM, Soares WR, Rodriguez DA, Camargo H, Riveros MP, Pabló AD (2013) Two contrasting severe seasonal extremes in tropical South America in 2012: flood in Amazonia and drought in northeast Brazil. J Clim 26(22):9137–9154

McSweeney C, Jones R (2010) Selecting members of the 'QUMP'perturbed-physics ensemble for use with PRECIS. Met Office Hadley Centre, Devon, UK 9

McSweeney CF, Jones RG, Booth BB (2012) Selecting ensemble members to provide regional climate change information. J Clim 25(20):7100

MoE (2011a) Climate action: adapting to change, protecting our future, 2011. Ontario Ministry of the Environment

MoE (2011b) Climate ready: Ontario's adaptation strategy and action plan, 2011–2014. Ontario Ministry of the Environment

Murphy JM, Sexton DM, Barnett DN, Jones GS, Webb MJ, Collins M, Stainforth DA (2004) Quantification of modelling uncertainties in a large ensemble of climate change simulations. Nature 430(7001):768–772

Murphy JM, Sexton DMH, Jenkins GJ, Booth BBB, Brown CC, Clark RT, Collins M, Harris GR, Kendon EJ, Betts RA, Brown SJ, Humphrey KA, McCarthy MP, McDonald RE, Stephens A, Wallace C, Warren R, Wilby R, Wood RA (2009) UK climate projections science report: climate change projections. Meteorological Office Hadley Centre

Nikulin G, Jones C, Giorgi F, Asrar G, Büchner M, Cerezo-Mota R, Christensen OB, Déqué M, Fernandez J, Hänsler A (2012) Precipitation climatology in an ensemble of CORDEX-Africa regional climate simulations. J Clim 25(18):6057–6078

NLWIS (2007) Daily 10 Km Gridded Climate Dataset: 1961–2003, Version 1.0. National Land and Water Information Service, Agriculture and Agri-Food Canada

Paerl HW, Paul VJ (2012) Climate change: links to global expansion of harmful cyanobacteria. Water Res 46(5):1349–1363

Piao S, Ciais P, Huang Y, Shen Z, Peng S, Li J, Zhou L, Liu H, Ma Y, Ding Y (2010) The impacts of climate change on water resources and agriculture in China. Nature 467(7311):43–51

Pielke RA, Wilby RL (2012) Regional climate downscaling: what's the point? Eos. Trans Am Geophys Union 93(5):52–53

Sanchez-Moreno JF, Mannaerts CM, Jetten V (2014) Influence of topography on rainfall variability in Santiago Island, Cape Verde. Int J Climatol 34(4):1081–1097

Schiermeier Q (2011) Increased flood risk linked to global warming. Nature 470(7334):316

Seager R, Naik N, Vogel L (2012) Does Global Warming Cause Intensified Interannual Hydroclimate Variability?*. J Clim 25(9):3355–3372

Senatore A, Mendicino G, Knoche HR, Kunstmann H (2014) Sensitivity of modeled precipitation to sea surface temperature in regions with complex topography and coastlines: a case study for the Mediterranean. J Hydrometeorol 15(6):2370–2396

Stocker T, Qin D, Plattner G-K, Tignor M, Allen SK, Boschung J, Nauels A, Xia Y, Bex V, Midgley PM (2014) Climate change 2013: the physical science basis. Cambridge University Press, Cambridge

Tam A (2009) Permafrost in Canada's subarctic region of Northern Ontario. University of Toronto, Toronto

Tebaldi C, Smith RL, Nychka D, Mearns LO (2005) Quantifying uncertainty in projections of regional climate change: a Bayesian approach to the analysis of multimodel ensembles. J Clim 18(10):1524–1540

Teutschbein C, Seibert J (2012) Bias correction of regional climate model simulations for hydrological climate-change impact

studies: Review and evaluation of different methods. J Hydrol 456:12–29

Themeßl MJ, Gobiet A, Heinrich G (2012) Empirical-statistical downscaling and error correction of regional climate models and its impact on the climate change signal. Clim Change 112(2):449–468

Trenberth KE (2011) Changes in precipitation with climate change. Clim Res 47(1):123

Um M-J, Yun H, Jeong C-S, Heo J-H (2011) Factor analysis and multiple regression between topography and precipitation on Jeju Island, Korea. J Hydrol 410(3):189–203

Wang X, Huang G, Lin Q, Nie X, Cheng G, Fan Y, Li Z, Yao Y, Suo M (2013) A stepwise cluster analysis approach for downscaled climate projection–A Canadian case study. Environ Model Softw 49:141–151

Wang LZ, Huang YF, Wang L, Wang GQ (2014a) Pollutant flushing characterizations of stormwater runoff and their correlation with land use in a rapidly urbanizing watershed. J Environ Informat 23(1):44–54

Wang X, Huang G, Lin Q, Liu J (2014b) High-resolution probabilistic projections of temperature changes over Ontario, Canada. J Clim 27(14):5259–5284

Wang X, Huang G, Lin Q, Nie X, Liu J (2014c) High-resolution temperature and precipitation projections over Ontario, Canada: a coupled dynamical-statistical approach. Q J R Meteorol Soc

Wang X, Huang G, Liu J (2014d) Projected increases in intensity and frequency of rainfall extremes through a regional climate modeling approach. J Geophys Res Atmos 119(23):13271–213286

Wang X, Huang G, Liu J (2014e) Projected increases in near-surface air temperature over Ontario, Canada: a regional climate modeling approach. Clim Dyn 141(689):1137–1146. doi:10.1002/qj.2421

Wang X, Huang G, Liu J, Li Z, Zhao S (2015) Ensemble projections of regional climatic changes over Ontario, Canada. J Clim. doi:10.1175/JCLI-D-15-0185.1

Wentz FJ, Ricciardulli L, Hilburn K, Mears C (2007) How much more rain will global warming bring? Science 317(5835):233–235

Wilby RL, Wigley T (1997) Downscaling general circulation model output: a review of methods and limitations. Prog Phys Geogr 21(4):530–548

Wilson S, Hassell D, Hein D, Morrell C, Tucker S, Jones R, Taylor R (2011) Installing and using the Hadley Centre regional climate modelling system, PRECIS

Yang C, Yu Z, Hao Z, Zhang J, Zhu J (2012) Impact of climate change on flood and drought events in Huaihe River Basin, China. Hydrol Res 43(1–2):14–22